Nanoscale

Accepted Manuscript

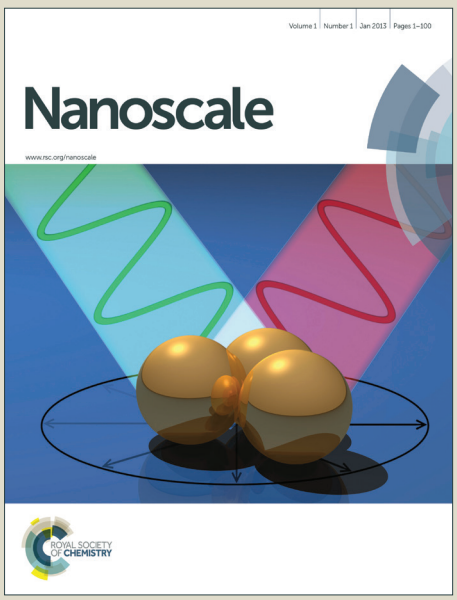

ROYAL SOCIETY OF CHEMISTRY

www.rsc.org/nanoscale

"Red-to-blue"colorimetric detection of cysteine via anti-etching of silver nanoprisms

Yonglong Li[a,b], Zihou Li[a], Yuexia Gao[a], An Gong[a], Yuejie Zhang[a], Narayan S. Hosmane[c], Zheyu Shen[a,*], Aiguo Wu[a,*]

[a]*Key Laboratory of Magnetic Materials and Devices, & Division of Functional Materials and Nano Devices, Ningbo Institute of Materials Technology & Engineering, Chinese Academy of Sciences, Ningbo, Zhejiang, 315201, China.*

[b]*Nano Science and Technology Institute, University of Science and Technology of China, Suzhou, Jiangsu, 215123, China.*

[c]*Department of Chemistry & Biochemistry, Northern Illinois University, DeKalb, IL 60115, USA.*

***Corresponding authors**

E-mail: aiguo@nimte.ac.cn; or shenzheyu@nimte.ac.cn

Tel: +86 574 86685039, or +86 574 87617278; Fax: +86 574 86685163.

The reported strategies for cysteine (Cys) colorimetric detection based on noble metal nanomaterials include triggering aggregation, ethcing or fluorescence quenching of the nanomaterials by Cys. In this study, we propose a new strategy for Cys colorimetric detection, i.e. anti-etching of silver nanoprisms (AgNPRs). In the absence of Cys, iodide ions (I^-) could etch the corners and edges of the AgNPRs and induce the morphology transition from nanoprism to nanodisk, which results in color change of the AgNPR dispersion from blue to red. In the presence of Cys, however, Cys can prevent the AgNPRs from I^- attack. In that case, the color of the AgNPR dispersion containing I^- and Cys remains blue. The mechanism is confirmed by using UV-vis spectra, TEM, DLS, Raman spectra and XPS spectra. According to the sensing effect of the Cys detection system, the concentration of I^- incubated with AgNPRs, incubation time of AgNPRs and I^-, and pH value of AgNPR dispersions are optimized to be 5.0 μM, 10 min and pH 6.2, respectively. At the optimized conditions, the proposed Cys detection system has excellent selectivity and high sensitivity. The limit of detection (LOD) of our Cys detection system is 25 nM by the naked eyes, which is much better than the reported lowest LOD by eye-vision (100 nM), and 10 nM by UV-vis spectroscopy. The results of Cys detection in rabbit urine or plasma samples reinforce that our Cys detection system is applicable for rapid colorimetric detection of Cys in real body fluid samples.

1. Introduction

Cysteine (Cys) is the only natural amino acid with -SH that widely exists in biological systems.[1] It plays an important role in human body by interacting with proteins intramolecularly through disulfide bonds in order to support their secondary structures that have numerous biological functions in metabolism.[1, 2] In addition, Cys is also a potential neurotoxin,[3] a biomarker for medical settings[4, 5] and a disease-associated physiological regulator.[6, 7] The conventional detection methods for Cys include fluorescence-coupled HPLC techniques,[8, 9] electrochemical analysis,[10-12] fluorescent dyes-based fluorometry[13-15] and chromatography.[16] Although most of them offer high sensitivity and multi-element analysis, they are relatively complicated (not suitable for on-site detection) and not cost-effective (time-consuming and costly). A suitable on-site analysis by a simple and rapid detection technique for Cys with high sensitivity and excellent selectivity is therefore sorely demanded.

In this context, rapid colorimetric detection methods, based on modified noble metal nanomaterials, should prove to be attractive tools because of their strong surface plasmon resonance (SPR) and their high extinction coefficient.[17-20] Until recently, many nanomaterials of noble metals, such as gold nanorods (AuNRs),[21, 22] gold nanoparticles (AuNPs),[23, 24] silver nanoparticles (AgNPs),[25] silver nanoprisms (AgNPRs)[26] and silver nanoclusters (AgNCs),[27, 28] have been found to detect Cys. The Cys detection mechanisms, involving these noble metal nanoparticles, included aggregation triggering,[22-25] etching[26] or fluorescence quenching.[27, 28] However, it should be emphasized that the aggregation, etching and/or fluorescence quenching of nanomaterials are not desirable properties, since these can be influenced by a number of external factors in real life applications. In order to achieve high selectivity, it is essential to make sure that the nanomaterials avoid aggregation, etching or fluorescence quenching during the Cys detection. To the best of our knowledge, little is known about the anti-etching of nanomaterials for Cys detection.

Herein, we propose a new strategy for Cys colorimetric detection, i.e. anti-etching of silver nanoprisms (AgNPRs), which is shown in Scheme 1. In the absence of Cys, iodide ions (I^-) could

attach to the corners and edges of the AgNPRs via Ag−I bond and etch the corners and edges, which results in morphology transition of the nanoparticles from nanoprism to nanodisk.[29] That's because the silver atoms at the corners and edges of AgNPRs are active and easy to coordinate with I^- ($K_{sp}$of AgI was 8.49×10^{-17}),[30] resulting in dissociation of the silver atoms from its original nanostructure.[31] The morphology transition from nanoprism to nanodisk induces an obvious color change of the AgNPR dispersion from blue to red. However, in the presence of Cys, the morphology transition of AgNPRs cannot be caused by I^- as Cys may act as a protective agent and increase the stability of silver atoms at the corners and edges avoiding the attack by I^- ions. In this scenario, the color of the AgNPR dispersion with I^- and Cys could remain blue. Therefore, due to the mechanism of anti-etching, Cys could be directly recognized by visualizing the color change of AgNPR dispersion containing I^- by the naked eyes with high sensitivity and excellent selectivity.

2. Experimental section

2.1 Materials

L-cysteine (Cys), L-histidine (His), L-lysine (Lys), L-arginine (Arg), L-threonine (Thr), L-glutathione (GSH), Hydrogen peroxide (H_2O_2), Silver nitrate ($AgNO_3$), Trisodium citrate dehydrate ($C_6H_5Na_3O_7\cdot2H_2O$), Sodium borohydride ($NaBH_4$), Hydrochloric acid (HCl) and Nitric acid (HNO_3) were obtained from Sinopharm Chemical Reagent Co., Ltd. (Beijing, China). Poly(vinylpyrrolidone) (PVP, MW~58000g/mol), Potassium iodide (KI), L-asparagine (Asn), L-glutamine (Gln), L-tyrosine (Tyr), L-serine (Ser), L-aspartic acid (Asp), L-glutamic acid (Glu), L-glycine (Gly), L-alanine (Ala), L-lysine (Lys), L-leucine (Leu), L-isoleucine (Ile), L-tryptophan (Trp), L-proline (Pro), L-methionine (Met), L-phenylalanine (Phe), 3-mercaptopropionic acid (MPA), Bovine serum albumin (BSA) were purchased from Aladdin-regent Co., Ltd. (Shanghai, China). Fetal calf serum (FBS) was purchased from Gibco (Grand Island, USA). All the chemical reagents were used as received without further purification. All glasswares were washed by aquaregia (HCl/HNO_3 =3:1 (v/v)) and then cleaned with Milli-Q water.

2.2 Instruments

Surface plasmon resonance (SPR) absorption data were recorded with an ultraviolet and visible spectrophotometer (UV-vis, PERSEE T10CS). Dynamic light scattering (DLS) data were obtained on Zetasizer Nano ZS instrumentation (Malvern Instruments Ltd.). Transmission electron microscopy (TEM) images were performed using a JEOL2100 microscope operating at an accelerating voltage of 200 KV. X-ray photon spectrometry (XPS) was performed using an AXIS Ultra DLD instrument with Mg Kα radiation as the X-ray source. Raman spectra were measured using a Reinshaw inVia Reflex spectrometer with a Spectron Laser System (Nd:YAG laser, excitation at 532 nm).

2.3 Synthesis of AgNPRs

The AgNPRs were prepared according to a published method.[32] Typically, aqueous solutions of $AgNO_3$ (20 mM, 0.5 mL), $C_6H_5Na_3O_7 \cdot 2H_2O$ (30 mM, 6.0 mL), PVP (0.7 mM, 6.0 mL), and H_2O_2 (30 wt%, 240 μL) were mixed with 99.5 mL of Milli-Q water in a beaker of 300 mL capacity and stirred vigorously at room temperature. After that, a 1.0 mL aqueous solution of fresh $NaBH_4$ (100 mM) was then rapidly added to the above mixture with stirring to generate a pale yellow colloid. After 30 min of reaction, the resulting colloid, that changed its color from pale-yellow to blue, was subsequently stored at 4 ^{o}C.

2.4 Sensing detection of Cys

In separate experiments, a 100 uL aqueous solution of Cys with different concentrations was added to 850 μL of the freshly prepared AgNPR dispersions, during which time the pH value of the resulting mixture changed from 4.4 to 9.3. Subsequently, a 50 μL aqueous solution of KI (ranging from 0.05 to 500 μM) was added to each mixture, which was then shaken well and equilibrated at room temperature to observe the color change. While the incubation time varied from 1.0 to 22.0

min, the corresponding SPR absorption data were recorded by using a UV-vis spectrophotometer.

2.5 Selective detection of Cys

The selectivity verification of the amino acids was accomplished by using the proposed protocol for Cys detection system, based on the AgNPRs, in a manner similar to the one described above. The concentrations of other amino acids, used in this investigation, were 100 times higher than that of Cys.

2.6 Detection of real samples

Real samples of the rabbit urine and plasma samples obtained from the animal experiment center of Ningbo University (China) were filtered through a 0.2 μm membrane after centrifugation, and then spiked with standard Cys solutions at certain concentrations as stock solutions. After that, the Cys was detected using the UV-vis spectroscopy as mentioned above.

3. Results and discussion

3.1 Mechanism of the Cys detection system based on AgNPRs

The proposed new mechanism for Cys detection, i.e. anti-etching of AgNPRs (Scheme 1), was verified by UV-vis, TEM and XPS etc.

As shown in Figure 1, the prepared AgNPR dispersion is blue and has obvious UV-vis absorption with peak wavelengths at 331, 475 and 706 nm. After being incubated with I^- for 10 min, the color of AgNPR dispersion changes from blue to red. In addition, the peak wavelength of the UV-vis absorption at 706 nm shifts to 503 nm (blue shift). However, in the presence of Cys, the AgNPR dispersion has no color change, even though it has been incubated with I^-. The UV-vis absorption curves of AgNPR dispersions with or without I^- incubation in the presence of Cys are almost same, and the peak wavelengths around 706 nm have no blue shift compared with that of the AgNPR dispersion without I^- and Cys (control), but have a tiny red shift resulting from slight aggregation of

the AgNPRs due to intermolecular hydrogen bond of Cys (Scheme 1). These results indicate that Cys can prevent the AgNPRs from I^- attack.

Figure 2 (a) shows TEM image of the AgNPRs without Cys and I^- (control). We tried to improve the quality of the synthesized AgNPRs by optimizing the synthesis conditions. Although the as-prepared sample contains AgNPRs and other shaped silver nanomaterials as shown in Figure 2 (a), most of the particles are nanoprisms. Figure 2 (b) shows TEM image of the AgNPRs incubated with I^-. It is obvious that the morphology of AgNPRs is nanoprism, but it transfers to be nanodisk after being incubated with I^-. Figure 2 (c) shows TEM image of the AgNPRs in the presence of Cys. Figure 2 (d) represents TEM image of the AgNPRs incubated with I^- in the presence of Cys. It is found that, in the presence of Cys, the morphology of AgNPRs is nanoprism, even after incubated with I^-. This result reconfirms the mechanism that Cys can act as a protective agent and increase the stability of silver atoms at the corners and edges, thus avoiding the attack of I^- (Scheme 1). From Figure 2 (c) and (d), it is clear that the AgNPRs aggregate in the presence of Cys caused by intermolecular hydrogen bond of Cys. This result is in agreement with that of the UV-vis absorption (Figure 1). The corresponding DLS results (Figure S1) confirm the etching of AgNPRs caused by I^-, along with the slight aggregation of AgNPRs induced by Cys.

Regarding the principle of the morphology transition of AgNPRs from nanoprism to nanodisk, it could be ascribed to that the active silver atoms at the corners and edges of AgNPRs are easy to be coordinated with I^- and separated from the original nanostructure.[31] Based on Gibbs-Thomson effect, a convex surface has a higher surface energy than a flat surface. In addition, the bottom and the side planes of the AgNPRs is {111} plane and {110} plane, respectively.[33] The silver atoms at the corner areas and the {110} facet have less coordination number than those at the {111} facet, which results in higher surface energy at these areas of the nanoprism.[31, 34] Therefore, the corners and edges of AgNPRs are more proneto be etched rather than other areas.

The Raman spectroscopyand XPS are supportive of the ability of Cys as a protective reagent, which stabilizes the silver atoms at the corners and edges during the interaction of AgNPRs with the

thiol groups of Cys. Figure S2 (a) and (b) show the Raman spectra of AgNPRs before and after incubation with I^-. The possible peak-shift at 237 cm^{-1} due to Ag–S stretch[35-37] is absent in both Figures S2 (a) and (b), but is clearly observable in Figures S2 (c) and (d), which are the Raman spectra of AgNPRs in the presence of Cys and AgNPRs incubated with I^- in the presence of Cys. This result indicates the adsorption of Cys molecules onto AgNPRs through stronger interaction between Ag and S (the K_{sp} of Ag_2S is 1.6×10^{-49})[38] than that between Ag and I (the $K_{sp}$of AgI is 8.49×10^{-17}).[30]

To further verify the interaction, XPS spectra were used to characterize the binding energies of Ag 3d and S 2p. Figure 3 (a) shows Ag 3d spectra of AgNPRs, AgNPRs in the presence of Cys, and AgNPRs incubated with I^- in the presence of Cys. It is found that the Ag 3d binding energy of AgNPRs is obviously different with that of the AgNPRs in the presence of Cys, but I^- has no influence on the Ag 3d binding energy. Figure 3 (b) shows S 2p spectra of Cys, AgNPRs in the presence of Cys, and AgNPRs incubated with I^- in the presence of Cys. Comparing with S 2p spectrum of the pure Cys, the latter two spectra have obvious shift indicating the interaction through the –SH groups and Ag atoms. AgNPRs and Cys have a little influence on I 3d spectra of KI (Figure S3) that may be a part of I^- absorption on the surface of the intermediate region of AgNPRs resulting in a small shiftinthe I 3d spectra, but it has no effect on the colorimetric detection of Cys.These results further demonstrate that AgNPRs can bemodified by Cys through Ag–S bond.

Furthermore, the influence of other molecules containing thiol moiety on Cys detection system has also been investigated. Figure 4 (a) shows the UV-vis absorption spectrum or image of AgNPR dispersion incubated with I^-(control), and Figure 4 (b, c, d, e) respectively imply that of AgNPR dispersion incubated with I^- in the presence of BSA, GSH, MPA or Cys. It is found that the UV-vis absorption spectrum and color of AgNPR dispersion in the presence of BSA or GSH are both similar with those of the control indicating no significant influence of BSA and GSH on our Cys detection system. However, the UV-vis absorption spectrum and color of AgNPR dispersion in the presence of MPA are very different with those of the control, but similar with those of Cys. That's

because MPA and Cys are both small molecules containing thiol group and can protect the AgNPRs from I^- attack, maintaining the original color and UV-vis absorption. Conversely, the molecular weight of GSH and BSA may be too large (GSH~307 Da, BSA~67 kDa) to touch the surface of AgNPRs due to the steric hindrance caused by the stabilizer trisodium citrate and PVP. Although MPA has interference on Cys detection, it does not influence the application of our proposed AgNPRs-based Cys detection system because MPA does not exist in a body.

3.2 Optimization of experimental conditions

The concentration of I^- incubated with AgNPRs, incubation time of AgNPRs and I^-, and pH value of AgNPR dispersions are optimized according to the sensing effect of our Cys detection system.

The color change and the wavelength shift (betweenthe peak wavelength of the AgNPR dispersion incubated with or without I^-) are negligible when the I^- concentration is 0.05 μM, become obvious when the I^- concentration is 0.5 μM, and become almost maximum when the I^- concentration is higher than 5.0 μM (Figure S4). Because excess I^-may reduce Cys sensitivity of the sensor, its optimal concentration is fixed at 5.0 μM in the following experiments.

It is noteworthy that the wavelength shift increases with increasing of the incubation time, and become almost constant when the incubation time is higher than 10 min (Figure S5), which is chosen as the optimal time in the following study.

Although the wavelength shift is highest for the experiment at pH 4.4, the color change of the AgNPR dispersions incubated with 5.0 μM of I^- in the presence of Cys (5.0 μM) compared with that in the absence of Cys (controls) become more and more obvious with increasing of pH value in the range of 4.4 to 6.2, and no further change in color or its wavelength shift could be observed when the pH value is higher than 6.2 (Figure S6). In addition, the pH values lower than 5.0 can induce conversion of the silver nanoprisms into nanodiscs.[39] Consequently, the pH value of 6.2 is fixed as an optimal pH in subsequent experiments.

3.3 Selectivity of the Cys detection system

The selectivity ofthe AgNPRs-based detection system for Cys is evaluated by comparing with other amino acids. The color of the AgNPR dispersions incubated with 5.0 μM of I^- in the presence of 500 μM of other amino acids is red like that in the absence of amino acid (control), but that in the presence of 5.0 μM of Cys is blue (Figure S7(a)). The UV-vis spectra of the AgNPR dispersions incubated with 5.0 μM of I^- in the presence of 500 μM of other amino acids is similar with that in the absence of amino acid (control), but very different with that in the presence of 5.0 μM of Cys (Figure S7(a)). Figure 5 (a) shows the wavelength shift between the peak wavelengths of the AgNPR dispersions incubated with 5.0 μM of I^- in the presence of single amino acid (the concentration is 5.0 μM for Cys, but 500 μM for other amino acids) and that in the absence of amino acid. It is found that the wavelength shift of Cys is much higher than that of other amino acids. These results demonstrate that only Cys could protect the AgNPRs from I^- attack, and the 100-fold excess other amino acids have no evident influence on the color and SPR band of the AgNPR dispersion.

The selectivity ofthe AgNPRs-based detection system for Cys is also verified by investigation of the influence of 100-fold excess other various amino acids on the Cys sensing effect. The color and UV-vis spectra of the AgNPR dispersions incubated with 5.0 μM of I^- in the presence of 5.0 μM of Cys and 500 μM of other amino acids are both similar with those of the AgNPR dispersions incubated with 5.0 μM of I^- in the presence of 5.0 μM of Cys (control, without other amino acids) (Figure S7(b)). Figure 5 (b) shows the wavelength shift between the peak wavelengths of the AgNPR dispersions incubated with 5.0 μM of I^- in the presence of amino acids (5.0 μM of Cys plus 500μM of other single amino acid) and that in the absence of amino acid. It is found that the wavelength shift in the presence of Cys and 100-fold excess other single amino acid is almost similar with that in the presence of Cys without other amino acid. These results indicate that 100-fold excess other various amino acids have no influence on the Cys sensing effect of our

AgNPRs-based detection system. Therefore, we can conclude that our proposed AgNPRs-based detection system exhibits excellent selectivity toward Cys, apparently due to the specific and strong thiol-Ag interaction.

3.4 Sensitivity of the Cys detection system

The colorimetric response and UV-vis spectra are used to evaluate the sensitivity of our proposed AgNPRs-based Cys detection system. The photographic image of the AgNPR dispersions incubated with 5.0 μM of I^- in the presence of Cys with various concentrations is shown in Figure6. We can find that the color of the AgNPR dispersion changes from red to blue with increasing of Cys concentration, and the limit of detection (LOD) by the naked eyes is 25 nM, which is better than those of other sensitive analytical methods[21-28] as shown in Table S1.

Figure7 (a) shows UV-vis absorption spectra of the AgNPR dispersions incubated with 5.0 μM of I^- in the presence of Cys with various concentrations. It is found that, with increasing of Cys concentration from 0 to 5.0 μM, the UV-vis absorption spectrum shifts towards red. That's because the morphology change of AgNPRs induced by I^- is prevented by Cys. Furthermore, the wavelength shift calculated between the peak wavelengths of the AgNPR dispersions incubated with I^- (5.0 μM) in the presence of Cys and that in the absence of Cys can be used for the quantitative analysis of Cys. Figure 7 (b) shows the plot of the wavelength shift as a function of Cys concentration ranging from 0 to 10 μM. The inset plot shows the wavelength shift versus different Cys concentrations in the range of 0.050-1.0 μM (R^2=0.9919). The good linear relationship indicates that our developed detection system can also be used for the quantitative analysis of Cys.

The above results demonstrate that our proposed detection system based on new mechanism of anti-etching of AgNPRs is applicable for rapid colorimetric detection and quantitative analysis of Cys with excellent selectivity and high sensitivity.

3.5 Detection of real samples

The proposed detection system is also applied for Cys detection in some real samples, such as fetal calf serum (FBS), rabbit urine and plasma samples. The UV-vis data are shown in Table S2. It is found that the detected Cys concentrations are relatively larger than that added. That's because Cys exists in the samples. The analysis in real samples of urine shows a systematic positive error. That's because the small molecules containing –SH group (e.g. mercapturic acid and homocysteine) may interfere the Cys detection. After dilution of the plasma, the detection result becomes better showing recovery close to 100%. These results reinforce that our Cys detection system is applicable for rapid colorimetric detection of Cys in real body fluid samples.

Although homocysteine (Hcy) is also present in biological fluids, our proposed sensor cannot distinguish cysteine from homocysteine (Figure S8). Therefore, our AgNPRs-based detection system can only detect the total amount of Hcy and Cys.

Because human body fluid contains high concentration of NaCl, we also tested the selectivity of the proposed method in the presence of a mixture of Cys and chloride ions. It can be seen that 0.9 % of NaCl has no influence on the Cys detection by our AgNPRs-based detection system (Figure S9).

As it is well known, HPLC is the reliable method for Cys determination. We determined the standard Cys solutions by HPLC with a C18 column. The flow rate is 1.0 mL/min. The mobile phase is a mixture of water and acetonitrile (95:5). A calibration curve is constructed with standard Cys solutions (Figure S10). It is found that the HPLC can only detect the Cys with a concentration larger than 1.0 μM. However, the linear range of our proposed method for cysteine detection is from 0.050 to 1.0 μM (Figure 7 (b)). Therefore, our proposed method is more sensitive than the existed HPLC method.

4. Conclusions

A simple method for Cys colorimetric detection is proven to be anti-etching of AgNPRs as presented here. The mechanism of anti-etching, i.e. preventing the corners and edges of AgNPRs from I^- attack, is confirmed by using UV-vis spectra, TEM, DLS, Raman spectra and XPS spectra.

According to the sensing effect of the proposed Cys detection system, the concentration of I^- incubated with AgNPRs, incubation time of AgNPRs and I^-, and pH value of AgNPR dispersions are optimized to be 5.0 μM, 10 min and pH 6.2, respectively. At the optimized experimental conditions, the selectivity of the AgNPRs-based detection system for Cys is evaluated by comparing with other amino acids. The results indicate that the selectivity of the AgNPRs-based detection system for Cys is excellent because Cys can protect the AgNPRs from I^- attack, but 100-fold excess other amino acids cannot. Additionally, the proposed AgNPRs-based detection system is highly sensitive for Cys. The LOD is 25 nM by the naked eyes, which is a new record for Cys detection by eye-vision, and 10 nM by UV-vis spectroscopy. We also find it's a good linear relationship (R^2=0.9919) between the wavelength shift and Cys concentration ranging from 0.050 to 1.0 μM. Our proposed detection system also exhibits satisfying performances to the rapid detection of Cys inreal body fluid samples (i.e. rabbit urine, plasma).

Acknowledge

This work was financially supported by Natural Science Foundation of China (Grants Nos. 31128007, 51203175), the Program of National High-Tech Program (863 Program No. SS2012AA063202), Hundred Talents Program of Chinese Academy of Sciences (2010-735), Zhejiang Provincial Natural Science Foundation of China (Grants No. R5110230, LQ13E030004), the aided program for Science and Technology Innovative Research Team of Ningbo Municipality (Grant No. 2009B21005). And the Project for Science and Technology Service of Chinese Academy of Sciences (KFJ-EW-STS-016).

References

1 E. Weerapana, C. Wang, G. M. Simon, F. Richter, S. Khare, M. B. D. Dillon, D. A. Bachovchin, K. Mowen, D. Baker and B. F. Cravatt, *Nature,* 2010, **468**, 790-795.

2 C. Jacob, G. I. Giles, N. M. Giles and H. Sies, *Angew. Chem., Int. Ed.,* 2003, **42**, 4742-4758.

3 M. Puka-Sundvall, P. Eriksson, M. Nilsson, M. Sandberg and A. Lehmann, *Brain Res.,* 1995, **705**, 65-70.

4 M. T. Goodman, K. McDuffie, B. Hernandez, L. R. Wilkens and J. Selhub, *Cancer,* 2000, **89**, 376-382.

5 J. Liu, H. C. Yeo, E. Övervik-Douki, T. Hagen, S. J. Doniger, D. W. Chu, G. A. Brooks and B. N. Ames, *J. Appl. Physiol.,* 2000, **89**, 21-28.

6 W. Dröge and Holm, E. *The FASEB J.,* 1997, **11**, 1077-1089.

7 N. Saravanan, D. Senthil and P. Varalakshmi, *Br. J. Urol.,* 1996, **78**, 22-24.

8 Y. V. Tcherkas and A. D. Denisenko, *J. Chromatogr. A,* 2001, **913**, 309-313.

9 V. Gazit, R. Ben-Abraham, C. G. Pick, I. Ben-Shlomo and Y. Katz, *Pharmacol. Biochem. Be.,* 2003, **75**, 795-799.

10 S. Shahrokhian, *Anal. Chem.,* 2001, **73**, 5972-5978.

11 A. Salimi and S. Pourbeyram, *Talanta,* 2003, **60**, 205-214.

12 G. Hignett, S.Threlfell, A. J. Wain, N. S. Lawrence, S. J. Wilkins, J. Davis, R. G. Compton and M. F. Cardosi, *Analyst ,* 2001, **126**, 353-357.

13 F. Tanaka, N. Mase and C. F. Barbas Iii, *Chem. Commun.,* 2004, **0**, 1762-1763.

14 M. Zhang, M. Yu, F. Li, M. Zhu, M. Li, Y. Gao, L. Li, Z. Liu, J. Zhang, D. Zhang, T. Yi and C. Huang, *J. Am. Chem. Soc.,* 2007, **129**, 10322-10323.

15 L. Shang, J. Yin, J. Li, L. Jin and S. Dong, *Biosens. Bioelectron.,* 2009, **25**, 269-274.

16 C. Lu, Y. Zu and V. W. W. Yam, *J. Chromatogr. A,* 2007, **1163**, 328-332.

17 F. Q. Zhang, L.Y. Zeng, Y. X. Zhang, H. Y. Wang and A. G. Wu, *Nanoscale,* 2011, **3**, 2150-2154.

18 L. Chen, X. Fu,W. Lu and L. Chen, *ACS appl. Mater. & interfaces.,* 2013, **5**, 284-290.

19 K. E. Fong and L. L. Yung, *Nanoscale,* 2013, **5**, 12043-12071.

20 Y. Xia, J. Ye, K. Tan, J. Wang and G. Yang, *Anal. Chem.,* 2013, **85**, 6241-6247.

21 P. K. Sudeep, S. T. S. Joseph and K. G. Thomas, *J. Am. Chem. Soc.,* 2005, **127**, 6516-6517.

22 H. Huang, X. Liu, T. Hu and P. K. Chu, *Biosens. Bioelectron.,* 2010, **25**, 2078-2083.

23 J. S. Lee, P. A. Ulmann, M. S. Han and C. A. Mirkin, *Nano Lett.,* 2008, **8**, 529-533.

24 J. Wang, Y. F. Li, C. Z. Huang and T. Wu, *Anal. Chim. Acta,* 2008, **626**, 37-43.

25 A. Ravindran, V. Mani, N. Chandrasekaran and A. Mukherjee, *Talanta,* 2011, **85**, 533-540.

26 T. Wu,Y. F. Li and C. Z. Huang, *Chin. Chem. Lett.,* 2009, **20**, 611-614.

27 L. Shang and S. Dong, *Biosens. Bioelectron.,* 2009, **24**, 1569-1573.

28 X. Yuan,Y. Tay, X. Dou, Z. Luo, D. T. Leong and J. Xie, *Anal. Chem.,* 2013, **85**, 1913-1919.

29 J. E. Millstone, W. Wei, M. R. Jones, H. Yoo and C. A. Mirkin, *Nano Lett.,* 2008, **8**, 2526-2529.

30 F. Qu, N. B. Li and H. Q. Luo, *Anal. Chem.,* 2012, **84**, 10373-10379.

31 J. An, B. Tang, X. Zheng, J. Zhou, F. Dong, S. Xu, Y. Wang, B. Zhao and W. Xu, *J. Phys. Chem. C,* 2008, **112**, 15176-15182.

32 G. S. Metraux, C. A. Mirkin, *Adv. Mater.,* 2005, **17**, 412-415.

33 R. Jin, Y. C. Cao, E. Hao, G. S. Metraux, G. C. Schatz and C. A. Mirkin, *Nature,* 2003, **425**, 487-490.

34 Z. L.Wang, *J. Phys. Chem. B,* 2000, **104**, 1153-1175.

35 H. I. S. Nogueira, *Spectrochim. Acta A,* 1998, **54**, 1461-1470.

36 X. C. Shen, H. Liang, J. H. Guo, C. Song, X.W. He and Y. Z. Yuan, *J. Inorg. Biochem.,* 2003, **95**, 124-130.

37 V. T. Joy and T. K. K. Srinivasan, *Spectrochim. Acta A,* 1999, **55**, 2899-2909.

38 X. C. Jiang and A. B.Yu, *Langmuir,* 2008, **24**, 4300-4309.

39 Y. Chen, C. Wang, Z. Ma, Z. Su, *Nanotechnology*, 2007, **18**, 325602-325606.

Captions

Scheme 1. Mechanism scheme of the AgNPR system for Cys detection. In the absence of Cys, I^- could attach to the corners and edges of AgNPRs via the Ag–I bond resulting in morphology transition from nanoprism to nanodisk. Cys can prevent I^- from attaching to the AgNPRs' surface and keep the shape frozen.

Figure 1. UV-vis spectra of the AgNPR dispersions at different conditions (the inset image corresponds to the colorimetric response). (a): AgNPRs (control); (b): AgNPRs incubated with 5.0 μM of I^-; (c):AgNPRs in the presence of Cys (5.0 μM); (d): AgNPRs incubated with 5.0 μM of I^- in the presence of Cys (5.0 μM).

Figure 2. TEM images of the AgNPRs at different conditions. (a): AgNPRs (control); (b): AgNPRs incubated with 5.0 μM of I^-; (c):AgNPRs in the presence of Cys (5.0 μM); (d): AgNPRs incubated with 5.0 μM of I^- in the presence of Cys (5.0 μM).

Figure 3. XPS spectra of the AgNPRs at different conditions. (a): Ag 3d of AgNPRs, AgNPRs in the presence of Cys (5.0 μM), AgNPRs incubated with 5.0 μM of I^- in the presence of Cys (5.0 μM); (b): S 2p of Cys, AgNPRs in the presence of Cys (5.0 μM), AgNPRs incubated with 5.0 μM of I^- in the presence of Cys (5.0 μM).

Figure 4. UV-vis absorption spectra of AgNPRs at different conditions. (a): AgNPRs incubated with 5.0 μM of I^- (control); (b): AgNPRs incubated with 5.0 μM of I^- in the presence of stabilizer BSA (5.0 μM); (c): AgNPRs incubated with 5.0 μM of I^- in the presence of stabilizer GSH (5.0 μM); (d): AgNPRs incubated with 5.0 μM of I^- in the presence of stabilizer MPA (5.0 μM); (e): AgNPRs incubated with 5.0 μM of I^- in the presence of stabilizer Cys (5.0 μM). The incubation time is 10 min. The inset image corresponds to the colorimetric response.

Figure 5. Selectivity of the AgNPRs-based detection system for Cys compared with other amino acids. (a): Wavelength shift between the peak wavelengths of the AgNPR dispersions incubated with 5.0 μM of I^- in the presence of single amino acid (the concentration is 5.0 μM for Cys, but 500 μM for other amino acids) and that in the absence of amino acid. (b) The wavelength shift between

the peak wavelengths of the AgNPR dispersions incubated with 5.0 μM of I^- in the presence of amino acids (5.0 μM of Cys plus 500 μM of other single amino acid) and that in the absence of amino acid.

Figure 6. Photographic image of the AgNPR dispersions incubated with 5.0 μM of I^- in the presence of Cys with various concentrations. The AgNPR dispersion incubated with 5.0 μM of I^- in the absence of Cys is used as a control.

Figure 7. (a) UV-vis absorption spectra of the AgNPR dispersions incubated with 5.0 μM of I^- in the presence of Cys with various concentrations. (b) Plot of wavelength shift as a function of Cys concentration ranging from 0 to 10.0 μM. The wavelength shift is calculated between the peak wavelengths of the AgNPR dispersions incubated with I^- (5.0 μM) in the presence of Cys and that in the absence of Cys. The inset plot shows the wavelength shift (mean±SD, n=3) versus different Cys concentrations in the range of 0.050-1.0 μM.

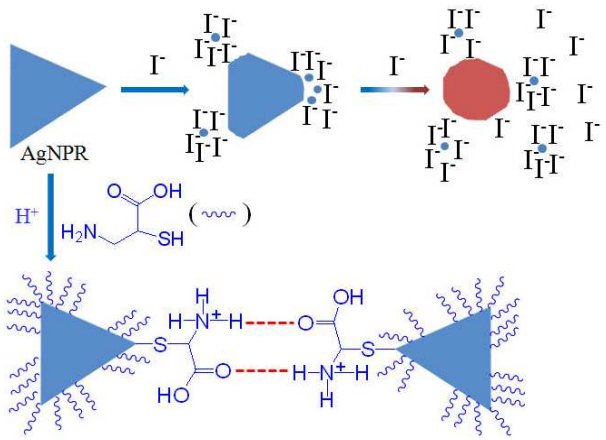

Scheme 1

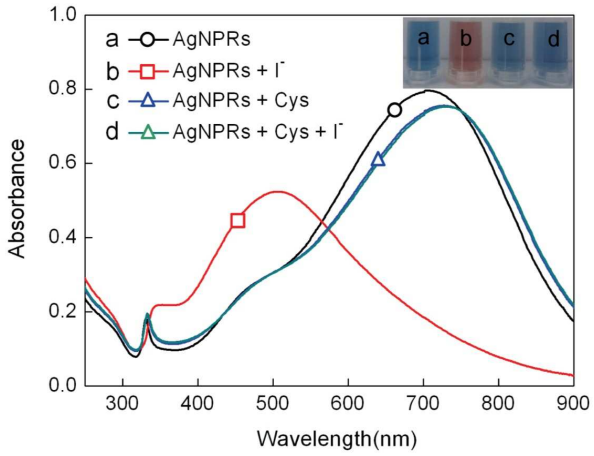

Figure 1

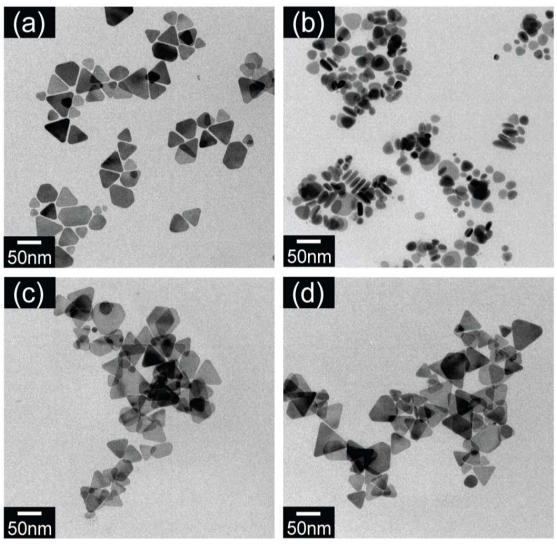

Figure 2

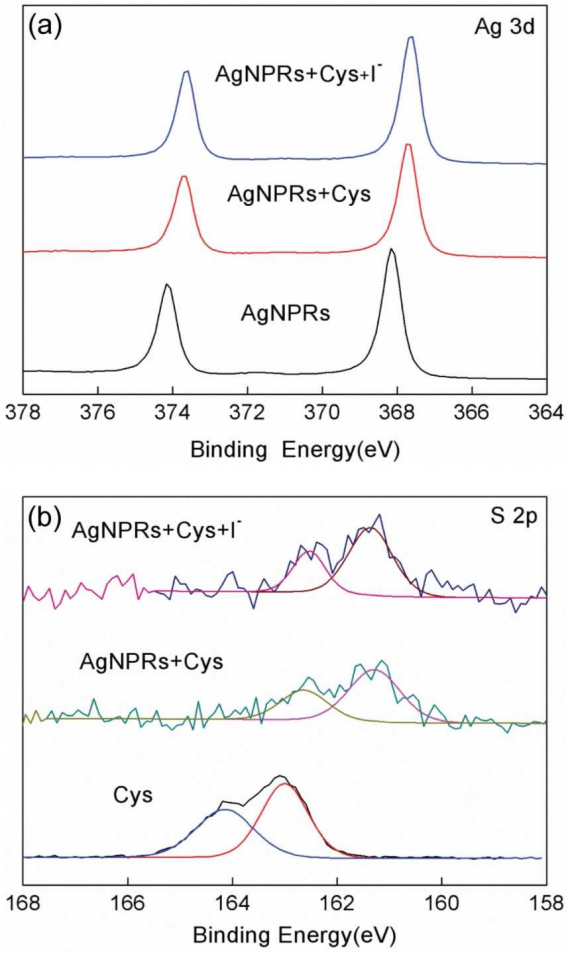

Figure 3

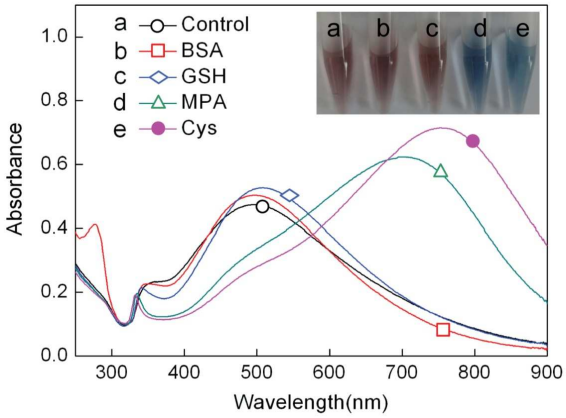

Figure 4

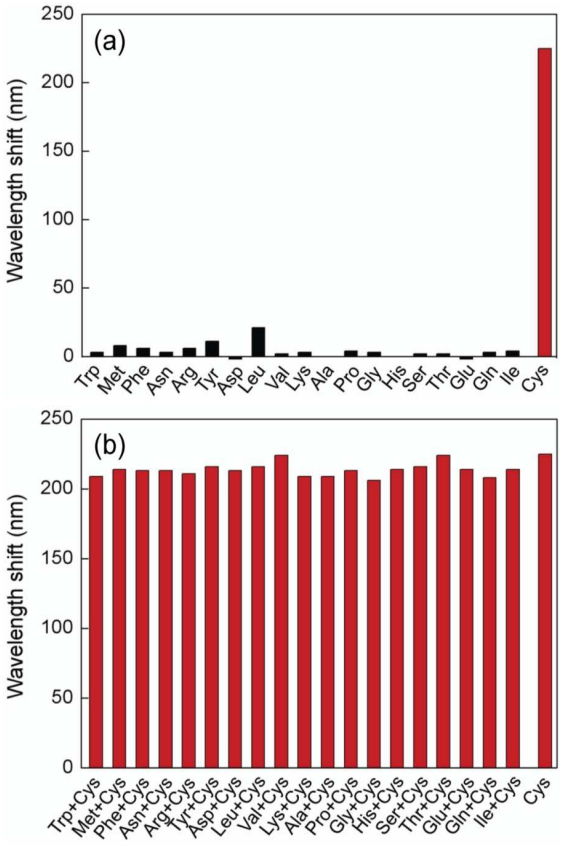

Figure 5

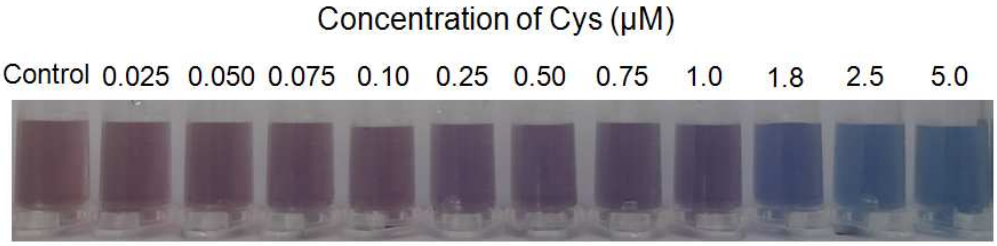

Figure 6

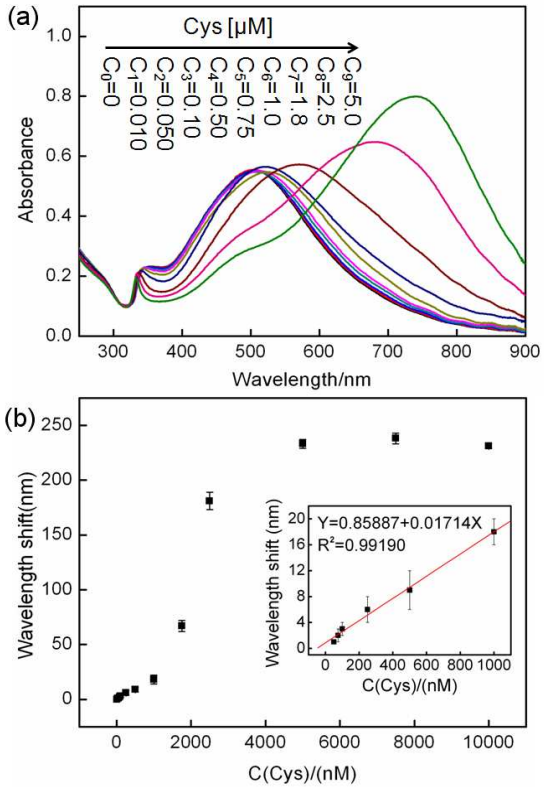

Figure 7

Graphical abstract

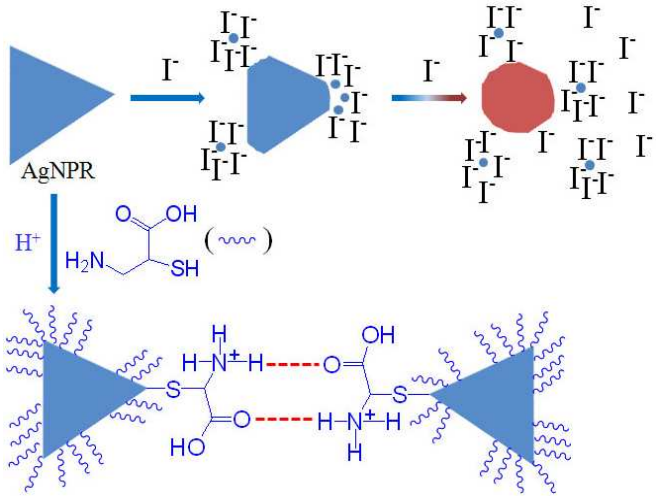

Mechanism scheme of the AgNPR system for Cys detection. In the absence of Cys, I^- could attach to the corners and edges of AgNPRs via the Ag–I bond resulting in morphology transition from nanoprism to nanodisk. Cys can prevent I^- from attaching to the AgNPRs' surface and keep the shape frozen.

Textual abstract

The reported strategies for cysteine (Cys) colorimetric detection based on noble metal nanomaterials include triggering aggregation, ethcing or fluorescence quenching of the nanomaterials by Cys. In this study, we propose a new strategy for Cys colorimetric detection, i.e. anti-etching of silver nanoprisms (AgNPRs). In the absence of Cys, iodide ions (I^-) could etch the corners and edges of the AgNPRs and induce the morphology transition from nanoprism to nanodisk, which results in color change of the AgNPR dispersion from blue to red. In the presence of Cys, however, Cys can prevent the AgNPRs from I^- attack. In that case, the color of the AgNPR dispersion containing I^- and Cys remains blue. The mechanism is confirmed by using UV-vis spectra, TEM, DLS, Raman spectra and XPS spectra. According to the sensing effect of the Cys detection system, the concentration of I^- incubated with AgNPRs, incubation time of AgNPRs and I^-, and pH value of AgNPR dispersions are optimized to be 5.0 μM, 10 min and pH 6.2, respectively. At the optimized conditions, the proposed Cys detection system has excellent selectivity and high sensitivity. The limit of detection (LOD) of our Cys detection system is 25 nM by the naked eyes, which is much better than the reported lowest LOD by eye-vision (100 nM), and 10 nM by UV-vis spectroscopy. The results of Cys detection in rabbit urine or plasma samples reinforce that our Cys detection system is applicable for rapid colorimetric detection of Cys in real body fluid samples.